# Pulse Width Modulation for Speeding Up Quantum Optimal Control Design

Qi-Ming Chen[1, 2] and Re-Bing Wu[†1, 2]

[1] *Department of Automation, Tsinghua University, Beijing, 100084, China*
[2] *Center for Quantum Information Science and Technology, TNList, Beijing, 100084, China*[*]

This paper focuses on accelerating quantum optimal control design for complex quantum systems. Based on our previous work [arXiv:1607.04054], we combine Pulse Width Modulation (PWM) and gradient descent algorithm into solving quantum optimal control problems, which shows distinct improvement of computational efficiency in various cases. To further apply this algorithm to potential experiments, we also propose the smooth realization of the optimized control solution, e.g. using Gaussian pulse train to replace rectangular pulses. Based on the experimental data of the D-Norleucine molecule, we numerically find optimal control functions in 3-qubit and 6-qubit systems, and demonstrate its efficiency advantage compared with basic GRAPE algorithm.



## I. INTRODUCTION

The idea of optimally controlling the dynamical behavior of microsystems described by quantum mechanics has been an explicit dream for more than 50 years [1]. Among all the approaches to solving the resulting optimization problems, model-based optimal control relies on computer simulations of quantum dynamics and numerical optimization algorithms [2]. The early attempt to seek the counterpart of the classical optimal control theory in quantum systems may be traced to Rabitz *et al.* [3], in which they explicated basic concepts of quantum optimal control theory which paved the way for later approaches. From then on, the studies have been enriched by numerous optimization algorithms with various applications.

Generally, a mathematical model of the underlying quantum system is required for designing optimal controls, and the strategies for solving this model-based optimization problem can be roughly divided into two classes. One approach is based on the necessary conditions derived from Pontryagin's Maximum Principle, i.e. "considering a pointer moving back and forth within the time interval" [2]. For that, Zhu, Sundermann, and Ho *et al.* proposed several quadratically convergent iterative algorithms [4–8]; Sklarz, Reich, and Schirmer *et al.* developed different kinds of Krotov algorithms [2, 9, 10]. The other approach is to eliminate the "Quantum Constrains", i.e. eliminating the equality constrain of Schrödinger equation (SE) and apply classical optimization algorithms [11, 12]. The quantum gradient algorithm was first introduced by Shi *et al.* based on difference method [13], and it was improved by Khaneja *et al.* through a much more convenient way for calculating the gradient, saying the Gradient Ascent Pulse Engineering (GRAPE) method [14]; besides, algorithms such as the Newton algorithm [15–17], quasi-Newton algorithm [18, 19], and various evolutionary algorithms [20] were also proposed.

The efficiency of model-based optimizations is usually determined by two factors. One is how fast the optimization algorithm can converge to the desired solution, and the other is how fast the dynamical evolution under a given control protocol can be calculated. In order to reduce the number of iterations, Ho *et al.* proposed the two-point boundary-value quantum control paradigm (TBQCP) [6–8], Eitan *et al.* combined the Krotov and quasi-Newton methods [21], and Watts *et al.* constructed a easily computable mathematical expression for the target function [22, 23]. More importantly, the simulation of quantum dynamical evolution need to be fast. Palao *et al.* restricted the objective to only the states used directly as registers [16, 17], Yip *et al.* proposed the concept of "propagation toolkit" to simplify control functions [24], Arai *et al.* introduced the reduced time-evolution operators [25].

In our previous work [26], we proposed the Pulse Width Modulation (PWM) method for efficiently simulating time-dependent systems. It transforms an arbitrary bandwidth-limited Hamiltonian into a sequence of on and off "Hamiltonian Pulses" (called Hamiltonian in PWM form), and reduces the simulation time by a large extent. In this paper, we design a gradient algorithm based on PWM and study the resulting improvement on the optimization efficiency with respect to multi-qubit quantum systems. The rest of this paper is organised as follows. Section II briefly reviews the PWM method, and Sec. III presents the problem, derives the optimization algorithm for one-control and multi-control cases. We apply the algorithm to 3-qubit and 6-qubit systems, and compare computational efficiency with the GRAPE algorithm in Sec. IV. We show how to smooth the optimized control function by example of transforming rectangular pulses into Gaussian pulse train in Sec. V. Finally, we summarise all the results and draw the conclusions in Sec. VI. In addition, App. A shows different realizations of PWM transformation and compares PWM with 2nd-order Split Operator Method (SPO), and App. B presents the detailed Hamiltonian for the D-Norleucine we used for numerical simulation.

[*] rbwu@tsinghua.edu.cn

## II. BRIEF REVIEW OF PWM

Pulse Width Modulation (PWM) is a well accepted concept in control technology in power electronics [27, 28], which is based on the fact that any function $u(t)$ with finite frequency bandwidth can be well approximated at any precision by a sequence of rectangular pulses with unanimous amplitude $\varepsilon = \max_t |u(t)|$ but different pulse width $t_p$. To apply PWM to a quantum system, we define the Frequency Band $\Delta = [\omega_{min}, \omega_{max}]$ as the interval from the minimum to the maximum frequency of all the time-dependent variables in the Hamiltonian, and the Frequency Scope $\Omega = M\omega_{min}$ as the frequency limit one should care about, where $M$ is called the Pulse Number within every time interval $2\pi/\omega_{min}$.

Consider an arbitrary time-dependent Hamiltonian in the semiclassical form

$$\hat{H}(t) = \hat{H}_0 + \sum_{i=1} u_i(t)\hat{H}_i, \tag{1}$$

where $H_0$ and $H_i$'s are time-independent Hamiltonians, $u_i(t)$'s are time-dependent real functions with finite bandwidth. The procedure of applying PWM in quantum system is based on Equal Integral Area Principle (EAP) [26]; in short, we divide every time interval $2\pi/\omega_{min}$ into $M$ pieces with equal length $\tau$, in each we replace $u_i(t)$ by a rectangular function with amplitude $\varepsilon_i$ and width $t_{p,i}^{(k)}$ which contains equal integral area. In this way, the time-dependent Hamiltonian is transformed into the PWM form

$$\hat{H}(t) = \hat{H}_0 + \sum_{i=1} s_i(t)\varepsilon_i\hat{H}_i, \tag{2}$$

where $s_i(t)$ is a sign function which switches among $0, \pm 1$; $\varepsilon_i \geq \max_t |u_i(t)|$ is a constant.

We further define anti-PWM transformation as transforming Eq. (2) into Eq. (1), which replaces rectangular pulse in each time interval $\tau$ by a constant with the same integral area; moreover, the Piecewise Constant (PWC) result may be further smoothed through EAP, which may be desired in many cases [5, 29]. However, as we will see the anti-PWM transform cannot always work well when one sets a relatively large time interval $\tau$ for simplifying the optimization in complex systems, how to smooth PWM pulses through smooth pulses would be discussed in Sec. V.

## III. ALGORITHM DESIGN

Consider an arbitrary time-dependent Hamiltonian in the form of Eq. (1), we name $u_i(t)$ as the $i$-th control signal, $\varepsilon_i$ as the bond on the $i$-th control field. Our aim is to tailor $u_i(t)$ to minimize the following defined objective IF at time $t = T$

$$\text{IF} = 1 - \frac{1}{2^m} Re\{tr\left[W^\dagger U(T,0)\right]\}, \tag{3}$$

where $W$ is the target operation, IF is called the "Infidelity" in quantum information [30].

Since optimizing the target Eq. (3) relays highly on the dynamics of the system, an efficient propagation scheme is crucial for quantum optimization. The broadly used approach is to break up the total evolution operator into small increments of duration $\tau$ in which the variation of the Hamiltonian operator is negligible, for example

$$\hat{U}(t+\tau, t) = \exp\Big[-i\tau(H_0 + u(t+\frac{\tau}{2})\hat{H}_1)\Big], \tag{4}$$

where the sampling point $t + \frac{\tau}{2}$ is decided by the Exponential Midpoint Rule that usually guarantees a result with the highest precision [31]. This approach is called the Piecewise Constant Scheme (PWC), which applies to nearly all the existing numerical quantum algorithms, e.g. the basic GRAPE algorithm [14].

However, PWM provides an alternative approach for solving SE, with the same simplicity but higher efficiency. Based on Eq. (2), one can construct a corresponding time-independent SE in each interval $\tau$ and combine the results to calculate the propagator, for example

$$\begin{aligned}\hat{U}_M(t+\tau, t) = \exp\Big[-it_f\hat{H}_0\Big] \exp\Big[-it_p(H_0 \pm \xi\hat{H}_1)\Big] \\ \times \exp\Big[-it_f\hat{H}_0\Big],\end{aligned}$$

where $t_p = \varepsilon^{-1}\int_t^{t+\tau} dt' u(t')$, $t_f = (\tau - t_p)/2$, subscript $M$ means it is calculated by PWM transformation.

Instead of using the amplitude of $u_i(t)$ as the decision variables of the system in GRAPE and all the other algorithms, the PWM approach utilizes the time intervals of rectangular pulses $t_{p,i}^{(k)}$ to be the decision variables. In the following, we derive the gradient formulas for combining PWM with the gradient descent algorithm.

### A. Gradient formula for one-control case

Consider a Hamiltonian with only one control function

$$H(t) = H_0 + u_x(t)H_x \ |u_x(t)| \leq \varepsilon_x,$$

we apply PWM transformation to the Hamiltonian and obtain the corresponding propagator of time $t = T$

$$U(T,0)=e^{-iH_0t_f^{(M)}}e^{-i\left(H_0+g^{(M)}H_x\right)t_p^{(M)}}\left(\prod_{k=1}^{M-1}e^{-iH_0\left(t_f^{(k)}+t_f^{(k+1)}\right)}e^{-i\left(H_0+g^{(k)}H_x\right)t_p^{(k)}}\right)e^{-iH_0t_f^{(1)}}.$$

where

$$g^{(k)}=\begin{cases}+\varepsilon_x, & \text{if the } k\text{-th pulse is positive}\\ -\varepsilon_x, & \text{otherwise}\end{cases}$$

is a hidden binary function which indicates whether the $k$-th pulse is positive or negative, $t_p^{(k)}$ is the time duration of the $k$-th pulses, and $t_f^{(k)}=\left(\tau-t_p^{(k)}\right)/2$. Note that the superscript turns out to be either $H_0$ or $H_0+g^{(k)}H_x$, in order to save computational resource we define

$$\begin{aligned}H_0&=D_0\Lambda_0D_0^\dagger,\\ H_0+g^{(k)}H_x&=D_x\Lambda_xD_x^\dagger,\end{aligned}\tag{5}$$

$$V_k=D_x\exp\left[-it_p^{(k)}\Lambda_x\right]D_x^\dagger,\tag{6}$$

$$\begin{aligned}U_1&=D_0\exp\left[-it_f^{(1)}\Lambda_0\right]D_0^\dagger\\ U_{k+1}&=\left\{D_0\exp\left[-i(t_f^{(k)}+t_f^{(k+1)})\Lambda_0\right]D_0^\dagger V_k\right\}U_k,\end{aligned}\tag{7}$$

where $k=1,\cdots,M-1$. Thus, we obtain the formula of the propagator and the corresponding gradient

$$\begin{aligned}U(T,0)&=D_0\exp\left[-it_f^{(k)}\Lambda_0\right]D_0^\dagger V_kU_k\\ \frac{\partial U(T,0)}{\partial t_p^{(k)}}&=\frac{-i}{2}U(T,0)\left(\left(V_kU_k\right)^\dagger H_x\left(V_kU_k\right)+U_k^\dagger H_xU_k\right)\end{aligned}\tag{8}$$

### B. Gradient formula for multi-control case

Consider a more general case where the Hamiltonian contains multiple control functions, e.g. the following 2-control case

$$H(t)=H_0+u_x(t)H_x+u_y(t)H_y,\ |u_{x,y}(t)|\le\varepsilon_{x,y}.$$

We define:

if $t_{p,x}^{(k)}-t_{p,y}^{(k)}\ge 0$:

$$\begin{aligned}t_a^{(k)}=t_{p,x}^{(k)},t_b^{(k)}=t_{p,y}^{(k)},t_d^{(k)}=\tfrac{t_{p,x}^{(k)}-t_{p,y}^{(k)}}{2},t_f^{(k)}=t_{f,x}^{(k)},\\ H_a^{(k)}=g_x^{(k)}H_x,H_b^{(k)}=g_y^{(k)}H_y;\end{aligned}$$

if $t_{p,x}^{(k)}-t_{p,y}^{(k)}\le 0$:

$$\begin{aligned}t_a^{(k)}=t_{p,y}^{(k)},t_b^{(k)}=t_{p,x}^{(k)},t_d^{(k)}=\tfrac{t_{p,y}^{(k)}-t_{p,x}^{(k)}}{2},t_f^{(k)}=t_{f,y}^{(k)},\\ H_a^{(k)}=g_y^{(k)}H_y,H_b^{(k)}=g_x^{(k)}H_x;\end{aligned}$$

where

$$g_i^{(k)}=\begin{cases}+\varepsilon_i, & \text{if the } k\text{-th pulse of } i\text{-th control is positive}\\ -\varepsilon_i, & \text{otherwise}\end{cases}$$

is a hidden binary function which indicates whether the $k$-th pulse of $i$-th control is positive or negative, $t_{p,i}^{(k)}$ for $i=x,y$ is the time duration of the $k$-th pulse of the $i$-th control, and $t_{f,i}^{(k)}=\left(\tau-t_{p,i}^{(k)}\right)/2$. In the similar way of one-control case, we obtain the corresponding propagator of time $t=T$

$$\begin{aligned}U(T,0)=&e^{-iH_0t_f^{(M)}}e^{-i(H_0+H_a)t_d^{(M)}}e^{-i(H_0+H_a+H_b)t_b^{(M)}}e^{-i(H_0+H_a)t_d^{(M)}}\\ &\times\Big(\prod_{k=1}^{M-1}e^{-iH_0\left(t_f^{(k)}+t_f^{(k+1)}\right)}e^{-i(H_0+H_a)t_d^{(k)}}e^{-i(H_0+H_a+H_b)t_b^{(k)}}e^{-i(H_0+H_a)t_d^{(k)}}\Big)e^{-iH_0t_f^{(1)}}.\end{aligned}$$

Similarly, we define

$$\begin{aligned}H_0&=D_0\Lambda_0D_0^\dagger,\\ H_0+H_a&=D_a\Lambda_aD_a^\dagger,\\ H_0+H_a+H_b&=D_b\Lambda_bD_b^\dagger,\end{aligned}\tag{9}$$

$$\begin{aligned}V_{k,1}&=D_a\exp\left[-it_d^{(k)}\Lambda_a\right]D_a^\dagger,\\ V_{k,2}&=D_b\exp\left[-it_b^{(k)}\Lambda_b\right]D_b^\dagger V_{k,1},\\ V_{k,3}&=V_{k,1}V_{k,2};\end{aligned}\tag{10}$$

$$\begin{aligned}U_1&=D_0\exp\left[-it_f^{(1)}\Lambda_0\right]D_0^\dagger,\\ U_{k+1}&=\left\{D_0\exp\left[-i\left(t_f^{(k)}+t_f^{(k+1)}\right)\Lambda_0\right]D_0^\dagger V_{k,3}\right\}U_k,\end{aligned}\tag{11}$$

where $k=1,\cdots,M-1$. Thus we obtain the formula of

the propagator and the corresponding gradient

$$U(T,0) = D_0 \exp\left[-it_f^{(k)}\Lambda_0\right] D_0^\dagger V_{m,3} U_m \tag{12}$$

$$\frac{\partial U(T,0)}{\partial t_a^{(k)}} = \frac{-i}{2} U(T,0)\left( (V_{k,3}U_k)^\dagger H_a (V_{k,3}U_k) + U_k^\dagger H_a U_k \right)$$

$$\frac{\partial U(T,0)}{\partial t_b^{(k)}} = \frac{-i}{2} U(T,0)\Big( (V_{k,2}U_k)^\dagger H_b (V_{k,2}U_k) + (V_{k,1}U_k)^\dagger H_b (V_{k,1}U_k) \Big)$$

### C. Algorithm design

Without loss of generality, we present the whole procedure for the algorithm according to the one-control case:

(0) Diagonalize the Hamiltonian $H_0$ and $H_0 + g^{(k)}H_x$ using Eq. (5), and guess the initial pulse intervals $t_p^{(k)}$.
(1) Calculate the exponents $V_k$ and $U_k$ using Eq. (6) and (7), the propagator and the gradient using Eq. (8).
(2) Evaluate $\partial U(T,0)/\partial t_p^{(k)}$ and update $t_p^{(k)}$ by gradient descent method (or other descent methods [11]).
(3) Evaluate the infidelity IF in Eq. (3) with these new $t_p^{(k)}$, repeat step (1)$\sim$(3) if the result is not satisfactory.
(4) Using anti-PWM transformation or smooth pulses to generate a smooth result.

Since Eq. (5) and (9) allow one to diagonalize and calculate the exponents previously (offline), it transforms the large number of calculations of exponents with matrices on the shoulder Eq. (4) into exponents with only scalars on the shoulder Eq. (8) and (12), which may simplify the computational complexity and accelerate the simulation of quantum dynamics by a large extent; moreover, Eq. (5)-(7) and Eq. (9)-(11) can be recycled in Eq. (8) and (12) for calculating the time evolution and the corresponding gradient. Thus, we may expected that PWM should be very efficient for solving optimization problems, especially in complex situations.

## IV. OPTIMIZATION EXAMPLES

Consider the example of D-Norleucine molecule which contains six homonuclear carbon spins that can be encoded as qubits for Nuclear Magnetic Resonance (NMR) quantum computation. The system's Hamiltonian reads [32, 33]

$$H(t) = H_0 + u_x(t)H_x + u_y(t)H_y,\ |u_{x,y}(t)| \le \varepsilon$$

where the complete form of $H_0$ and $H_{x,y}$ are given in App. B, $u_{x,y}(t)$ are the control functions implemented by radio-frequency magnetic fields, $\varepsilon = 2$MHz is the bound on the amplitude of control fields.

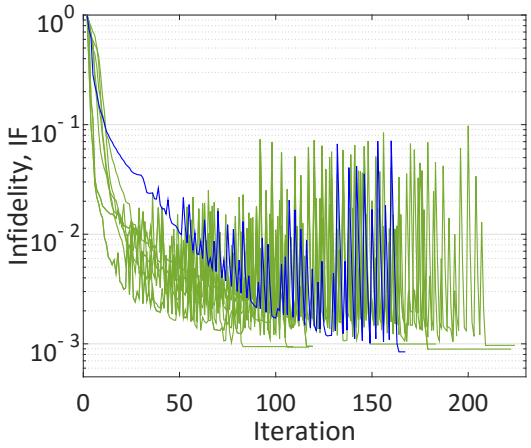


FIG. 1. (Color online) The infidelity IF of the PWM pulses with the iteration number in the optimization procedure from 10 randomly chosen fields, for the gate control over $C_1$, $C_2$, and $C_3$ with accuracy requirement IF $\le 1\times10^{-3}$ and $M = 1\times10^5$.

### A. 3-qubit example with single control

To illustrate how the PWM algorithm works, we choose the first three nuclears $C_1$, $C_2$, $C_3$ to seek an optimal solution. The target operation is to realize an $\frac{\pi}{2}$-rotation on $C_1$ around the $\langle\sigma_x\rangle$-axis at time $T = 10ms$ while remain the rest spins unchanged, saying

$$W = \exp\left(-i\frac{\pi}{4}\sigma_x\right)\otimes I^2,$$

where $I$ is identity.

We start from 10 randomly chosen initial fields of $u(0)$, set $M = 1\times10^5$ to transform the Hamiltonian into the PWM form, and apply the gradient optimization algorithm to look for optimal solutions. Since there is no guarantee that the algorithm will converge to the global minimum [14], we add some random perturbations on the gradient to try to avoid potential trap. Figure 1 shows the corresponding results, where all the 10 cases achieve the infidelity requirement IF $\le 1\times10^{-3}$ within 210 iterations. The blue line corresponds to a typical optimization procedure that achieves IF $= 0.84\times10^{-3}$ after 164 iterations, where the infidelity could be extremely close to zero under the same condition when we allow more iterations, or when we apply a more sophisticated algorithm (such as the genetic algorithm). This indicates that the PWM algorithm is capable of finding highly accurate optimal solutions.

Since a continuous control field is more acceptable than a rectangular one in laboratory, we reverse the PWM transformation procedure to convert the optimized PWM control field back to the continuous field. Figure 2(a) and 2(b) respectively show the corresponding continuous control field $u(t)$ in time domain and frequency domain, which slightly increases the infidelity but still guarantees

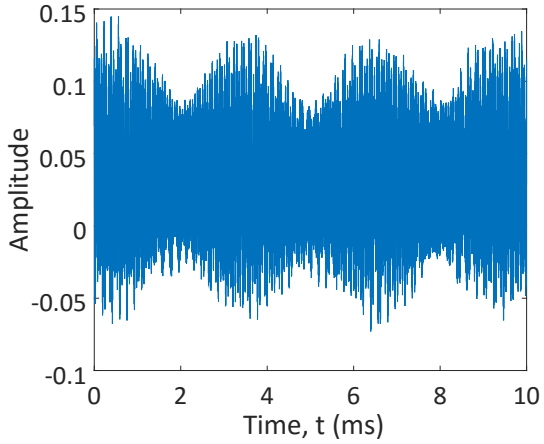


(a)

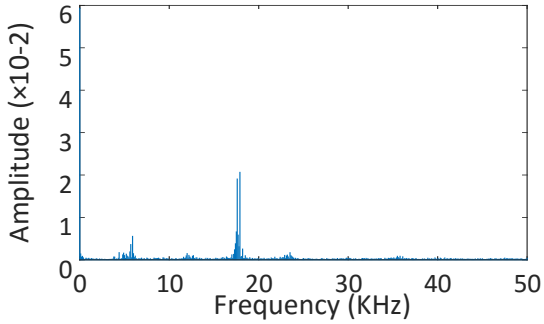


(b)

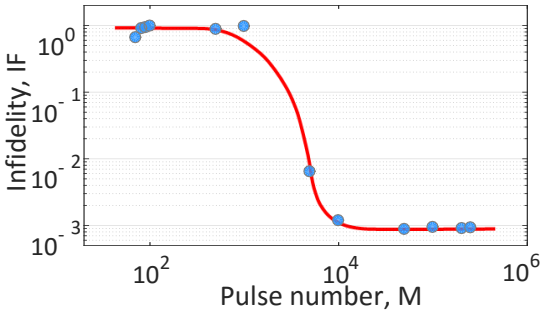


(c)

FIG. 2. (Color online) The PWM optimized continuous field (a) in the time domain and (b) in the frequency domain, for the gate control over $C_1$, $C_2$, and $C_3$ with accuracy requirement IF $\leq 1 \times 10^{-3}$ and $M = 1 \times 10^5$; (c) Infidelity IF of continuous control fields, which are transformed from those optimized PWM pulses with different pulse number $M$. The red line is fitted by the numerical samples (blue dots).

a rather high control precision IF $= 0.95 \times 10^{-3}$. To test the performance of the continuous control fields transformed from PWM pulses with different parameter $M$, we vary $M$ from 50 to $2.5 \times 10^5$ to optimize the same problem and anti-transformed the optimized PWM pulses into continuous fields. Figure 2(c) reveals the relation between the performance of the continuous

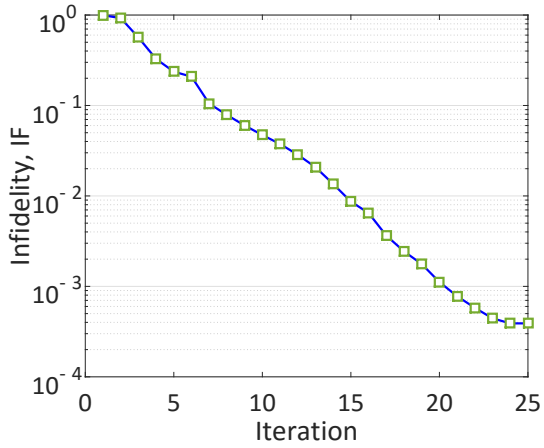


FIG. 3. (Color online) Infidelity (IF) of the PWM pulses with the iteration number in the optimization procedure from 10 randomly chosen fields, for the gate control over the whole 6 spins with $M = 1 \times 10^5$. The algorithm ceases at IF $= 3.89 \times 10^{-4}$ after 24 iterations.

control field and the pulse number $M$ of the optimization process. We found that the anti-transformed fields could still provide a rather accurate result if the PWM time interval $\tau \leq 1\mu s$ ($M \geq 1\times10^4$) for this problem; however, it is very difficult to obtain a satisfactory continuous field when $\tau \geq 1\mu s$ ($M \leq 1 \times 10^4$). This can be explained by that EAP works under the condition of small time interval $\tau$, for it is equivalently using only the 1st-order term of Magnus expansion [26]. Nevertheless, since in the latter case the time interval $\tau$ for preparing each pulse is relatively long, directly using on and off pulses may be applicable in contemporary laboratory conditions. On this regard, one may think the results for small pulse number $M$ is still acceptable, which further saves the optimization procedure by a large extent.

### B. 6-qubit example with 2 controls

We consider a larger system with two control functions for manipulating all the six spins in the molecule, which is regarded to be very difficult for seeking optimal solutions [34]. The target operation is to realize the CNOT gate on $C_1$ and $C_2$ at time $T = 10s$ while remain the rest spins unchanged, saying

$$W = U_{CNOT} \otimes I^4,$$

where $I$ is identity. The time duration may touch the limit of the dephasing time in many NMR systems; nevertheless, it can be achieved in well-prepared samples and in a good experimental apparatus at reasonably high magnetic fields [30]. In this regard, we still focus on seeking optimal control solutions in closed systems.

We start from a randomly chosen initial fields of $u(0)$, set $M = 1 \times 10^5$ to transform the Hamiltonian into

the PWM form, and apply the gradient optimization algorithm to look for optimal solutions. Figure 3 shows the optimization procedure which achieves the infidelity IF $= 3.89 \times 10^{-4}$ after 24 iterations. We further changed other target operations and also met no any trap in the optimization process, which is consistent with the landscape of quantum system from the practical perspective, saying the traps of optimization are usually avoidable when the time duration is very long [35]. On the other hand, the PWM algorithm achieves a very high precision with only 24 iterations. It reveals that PWM is highly efficient to handle high dimension, high accuracy, and long time interval problems which are regarded as rather difficult for other algorithms [34].

### C. Efficiency analysis

PWM speeds up quantum optimal control in accelerating the simulation of quantum dynamical evolution. To quantitatively compare the optimization efficiency of basic GRAPE algorithm and PWM based gradient algorithm, we suppose the iterations before achieving the target are of the same scale for the two algorithms, and compare the CPU time $t_c$ of the two method for calculating a desired propagator $U(T,0)$ [36]. For simplicity, we consider the 1-control case, use the Hamiltonian of 6-qubit example, and set the desired control function $u(t) = \sin(\omega t)$ for $\omega = 50$KHz.

Figure 4 displays the relation among the frequency scope $\Omega$ (which corresponds to pulse number $M$), time duration $t$, and the computational efficiency (CPU time $t_c$). Roughly speaking, PWM shows a distinct advantage in saving computational resources, at $T = 20\mu s$, IF $= 1\times10^{-1}$ the PWM algorithm saves 29.6% computational time for corresponding evolution; at $T = 200\mu s$, IF $= 1\times10^{-8}$ the PWM algorithm saves 29.7% computational time. Though compared with the low-dimensional results the computation advantage becomes more and more small with the increase of system dimension [26], PWM still shows a nearly 30% time saving in the 6-qubit system. Since a quantum optimization problem usually requires solving SE many times, and solving that for high-dimensional problems needs extremely long computation time, the 30% time saving in fact saves a large quantity of computational resources and makes it possible for optimizing complex systems.

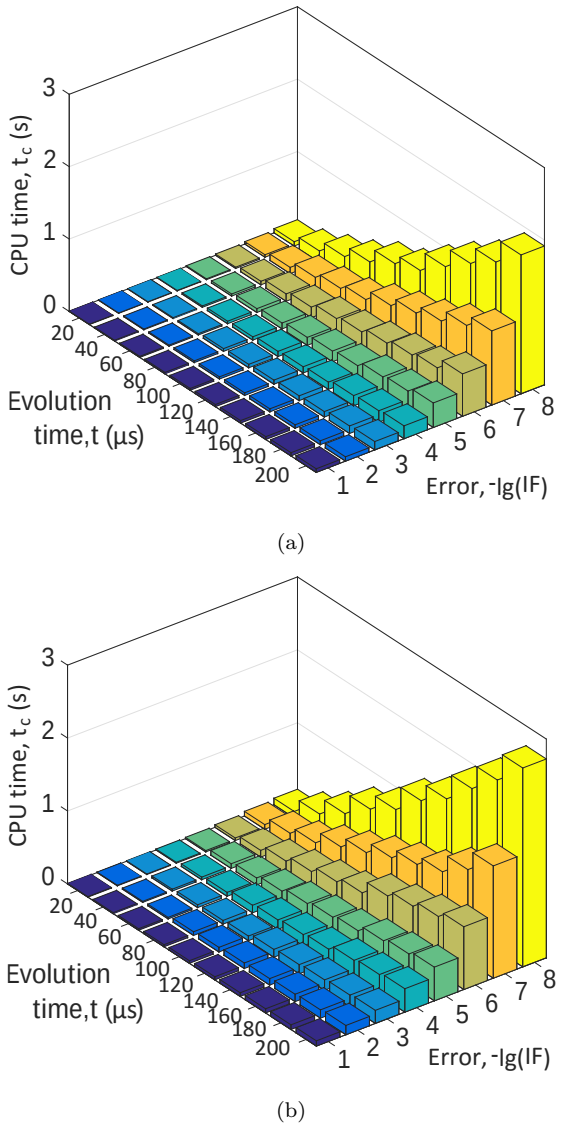


FIG. 4. (Color online) CPU time $t_c$ of the basic GRAPE algorithm (a) and the PWM algorithm (b) for calculating evolution $U(T,0)$ over the whole 6 spins at different time duration $T \in [20, 200]$ $\mu s$ and infidelity $-\lg(\text{IF}) \in [1, 8]$.

## V. SMOOTH PWM PULSES

Though we have demonstrated that PWM has the ability to efficiently find optimal controls in very complex systems, a smooth control is usually preferable in experimental realization such as superconducting control system [29] or laser control system [5, 37]. Typically, this mission is implemented by introducing a smooth error function into the objective, and re-optimize the control problems [5, 29]; however, the way to smooth PWM pulses is more straight forward, and this approach may be also applied to smoothing results from other algorithms.

The first approach is using anti-PWM transformation, which replaces rectangular pulse by a continuous function with the same integral area in each time interval $\tau$. This approach also meets the conclusion in [29], where the author found "the target fidelity does not depend on the shape of the pulse" for the subspace-selective self-adaptive differential evolution algorithm (SuSSADE). Since the number of control parameters are equal, one may smooth the piecewise constant control field by using EAP and obtain the same continuous field, rather than sacrifice the efficiency by introducing the error function.

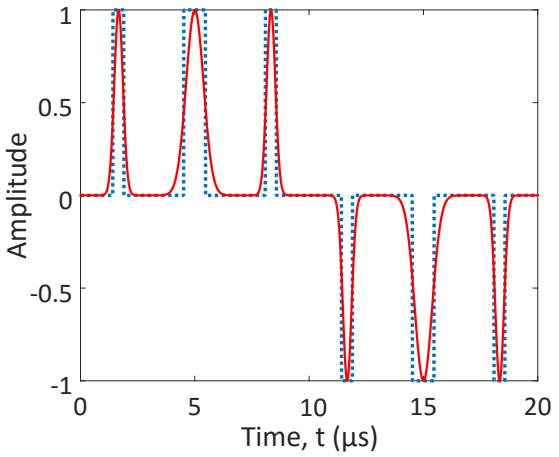


(a)

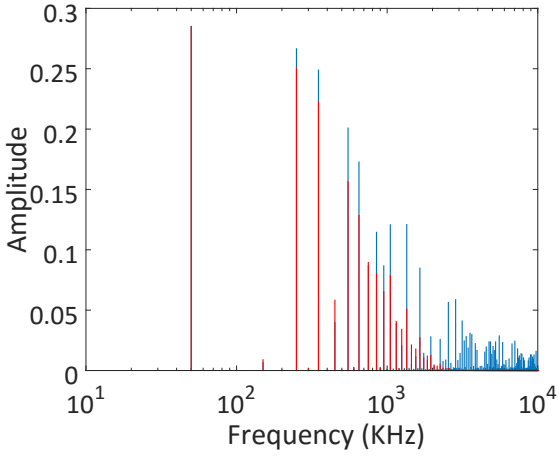


(b)

FIG. 5. (Color online) (a), (b) PWM pulses in rectangular form (blue) and in Gaussian form (red) in the time domain and in the frequency domain, respectively.

In fact, as we demonstrated in Sec. II the anti-transformation does not always work when one sets a relatively large $\tau$. Here, we propose another approach for smoothing PWM pulses; that is, we transform the rectangular pulses into continuous pulses, e.g. Gaussian pulses. Detail discussion of this can be found in [26]; in short, the rectangular pulses can be well approximated by a sequence of Gaussian pulses $\exp\left[-\pi t^2/t_p^2\right]$ with the same value of $t_p$. Figure 5(a) shows the relation between the rectangular pulses and the corresponding Gaussian pulses in time domain, Fig. 5(b) reveals the properties of the twos in frequency domain. It demonstrates the Gaussian pulses can well approximate the PWM pulses within a large frequency band. However, though the Gaussian pulse works for a relatively larger $\tau$, it does not always work also. How to effectively smooth PWM pulses is still an open problem for further discussions.

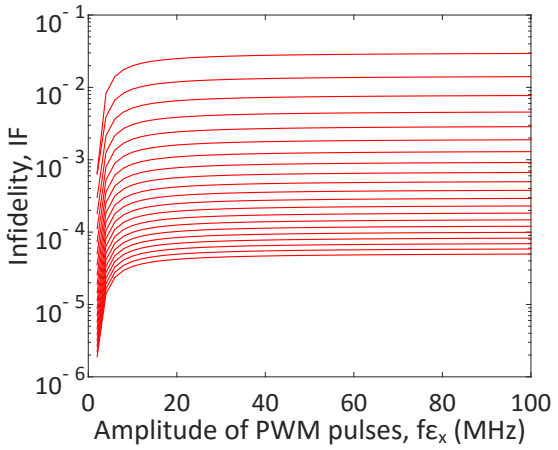


FIG. 6. (Color online) Infidelity (IF) of the PWM pulses with the amplitude of PWM pulses $f\varepsilon_x$ for calculation propagator $U(T,0)$ over the whole 6 spins at $T = 20\mu s$, where each line corresponds to different $M$ ($M \in [10, 50]$ increases from the top to the bottom, step by 2).

## VI. CONCLUSIONS

Combining Pulse Width Modulation (PWM) and gradient algorithm, we applied PWM into quantum optimal control problems. Compared with the basic GRAPE algorithm, the our algorithm raised the efficiency by a large extant, which provides us a highly efficient way for solving various optimization problems. In fact, PWM can also be imbedded in other descendent algorithms, such as Newton algorithm, quasi-Newton algorithm, and various evolutionary algorithms. In addition, since we have demonstrated in [26] that the rectangular pulses generated by PWM are rather robust with noise and can also be implemented by other functions (e.g. the Gaussian pulse train), it indicates the result of PWM algorithm may be directly applied into experiments. Thus, the PWM algorithm may highly simplify the current experiment relying on subtle control of shaped pulses, and provide a very robust and reliable quantum optimal control design.

## ACKNOWLEDGEMENTS

This work is supported by the National Natural Science Foundation of China (Grants No. 61134008, No. 61374091, and No. 91221205). We thank Professor Herschel Rabitz from Princeton University for useful discussions.

### Appendix A: Other forms of PWM pulses

According to the EAP, one may find there may be various ways for generating PWM pulses. In other words,

two Hamiltonians in the PWM form are identical within the frequency scope $\Omega$ as long as

$$t_{p,1}\varepsilon_{x,1} = t_{p,2}\varepsilon_{x,2},$$

where $t_{p,k}$ for $k = 1, 2$ represents the time duration of the pulses in the $k$-th Hamiltonian, $\varepsilon_{x,k}$ are the control amplitudes of the corresponding PWM pulses which can be virtually varied for computational simulation. For example, we can raise the pulse amplitude by $f$ and shrink the pulse duration $t_{p,k}$ by $1/f$, and keep the frequency properties of PWM pulse within $\Omega$ unchanged.

Figure 6 shows the relation between $f\varepsilon_x$ and the infidelity IF, where we consider the 1-control case, use the Hamiltonian of 6-qubit example, and set $u(t) = \sin(\omega t)$ for $\omega = 50KHz$ for calculating propagator $U(T, 0)$ for $T = 20\mu s$. On one hand, the infidelity IF increases slightly but still remains at a very small value when we raise the control amplitude $\varepsilon_x$ by $f$ times and shrink the pulse duration $t_p$ by $1/f$ times. On the other hand, it indicates the optimal choice for choosing the control amplitude is $\varepsilon_x = \max|u_x(t)|$. Since the Hamiltonian of the PWM form converges to the exactly form of the 2-order Split Operator method (SPO) in [38] when $\varepsilon_x$ goes to infinity, we may conclude that the PWM transformation always provides a much accuracy result than the SPO method [26].

Also, one can shift all the pulses by a small time shift and still keep the frequency properties (nearly) unchanged within the scope. Thus, one may raise the pulses of the $i$-th control field by $f$, shrink the pulse duration $t_{p,i}$ by $1/f$, and shift these pulses by $(1-m)\tau/2$ where $m$ stands for the number of different control fields while keep the evolution propagator $U(T, 0)$ almost unchanged. This provides one way to separately design the PWM pulses for different controls $u_k(t)$'s; that is, the generated PWM pulses make the controls act one-by-one in circle without any overlap. For convenience, we briefly give the gradient formula for the case of 2-controls in the following without proving:

$$\begin{aligned} H_0 &= D_0\Lambda_0 D_0^\dagger, \\ H_0 + g_x^{(k)}H_x &= D_x\Lambda_x D_x^\dagger, \\ H_0 + g_y^{(k)}H_y &= D_y\Lambda_y D_y^\dagger; \end{aligned} \tag{A1}$$

$$\begin{aligned} V_{k,1} &= D_0 \exp\Big[-i\Big(t_{f,x}^{(k)} + t_{f,y}^{(k)}\Big)\Lambda_0\Big] D_0^\dagger \\ &\quad \times D_x \exp\Big[-it_{p,x}^{(k)}\Lambda_x\Big] D_x^\dagger, \\ V_{k,2} &= D_y \exp\Big[-it_{p,y}^{(k)}\Lambda_y\Big] D_y^\dagger; \end{aligned} \tag{A2}$$

$$\begin{aligned} U_1 &= D_0 \exp\Big[-it_{f,x}^{(1)}\Lambda_0\Big] D_0^\dagger, \\ U_{k+1} &= \Big(D_0 \exp\Big[-i\Big(t_{f,x}^{(k+1)} + t_{f,y}^{(k)}\Big)\Lambda_0\Big] D_0^\dagger V_{k,2}V_{k,1}\Big) U_k; \end{aligned} \tag{A3}$$

| | $C_1$ | $C_2$ | $C_3$ | $C_4$ | $C_5$ | $C_6$ |
|---|---|---|---|---|---|---|
| $C_1$ | 17662 | | | | | |
| $C_2$ | 53.9 | 5382.4 | | | | |
| $C_3$ | 0.8 | 33.96 | 4006.7 | | | |
| $C_4$ | 2.47 | 0 | 33.96 | 2435.8 | | |
| $C_5$ | 0 | 3.03 | 0 | 34.73 | 2216.6 | |
| $C_6$ | 0 | 2.42 | 0 | 34.93 | 0 | 2105.8 |

TABLE I. The chemical shifts $\delta_k\omega_0/2\pi$ (diagonal elements, in unit of Hz) and coupling strengths $J_{jk}$ (off-diagonal elements, in unit Hz) of the carbon spins in D-Norleucine (CAS NO: 327-56-0). The data are experimentally obtained and provided by University of Science and Technology of China (unpublished).

$$\begin{aligned} U(T, 0) &= D_0 \exp\Big[-it_{f,y}^{(k)}\Lambda_0\Big] D_0^\dagger V_{k,2}V_{k,1}U_k \\ \frac{\partial U(T,0)}{\partial t_{p,x}^{(k)}} &= \frac{-i}{2}U(T,0)\Big(\left(V_{k,1}U_k\right)^\dagger H_x \left(V_{k,1}U_k\right) + U_k^\dagger H_x U_k\Big) \\ \frac{\partial U(T,0)}{\partial t_{p,y}^{(k)}} &= \frac{-i}{2}U(T,0)\Big(\left(V_{k,2}V_{k,1}U_k\right)^\dagger H_y \left(V_{k,2}V_{k,1}U_k\right) \\ &\quad + \left(V_{k,1}U_k\right)^\dagger H_y \left(V_{k,1}U_k\right)\Big). \end{aligned} \tag{A4}$$

## Appendix B: Hamiltonian of the selected carbon spins in the D-Norleucine molecule

Consider $m$ spins of the six and ignore their couplings to the remaining spins. The drift and control Hamiltonians are as follows:

$$\begin{aligned} H_0 &= \hbar\sum_{k=1}^{m}\delta_k\omega_0 S_z^k \\ &\quad + 2\pi\hbar\sum_{1\le j<k\le m} J_{jk}(S_x^jS_x^k + S_y^jS_y^k + S_z^jS_z^k), \\ H_{x,y} &= -\hbar\varepsilon\sum_{k=1}^{m}(1-\delta_k)S_{x,y}^k, \end{aligned}$$

where

$$S_{x,y,z}^k = \frac{1}{2}I_2^{\otimes(k-1)} \otimes \sigma_{x,y,z} \otimes I_2^{\otimes(m-k)}$$

are spin operators act on the $k$-th spin, $\otimes$ represents the Kronecker product, $\sigma_{x,y,z}$ represent the standard Pauli operators. The chemical shift $\delta_k\omega_0$ of each spin and $J$-coupling constants $J_{jk}$ between them are listed as the diagonal and off-diagonal elements in TABLE I.

[1] W. S. Warren, H. Rabitz, and M. Dahleh, Science **259**, 1581 (1993).

[2] S. G. Schirmer and P. de Fouquieres, New Journal of Physics **13**, 073029 (2011).

[3] A. P. Peirce, M. A. Dahleh, and H. Rabitz, Phys. Rev. A **37**, 4950 (1988).

[4] W. Zhu, J. Botina, and H. Rabitz, The Journal of Chemical Physics **108**, 1953 (1998); W. Zhu and H. Rabitz, *ibid.* **109**, 385 (1998).

[5] K. Sundermann and R. de Vivie-Riedle, The Journal of Chemical Physics **110**, 1896 (1999).

[6] T. S. Ho and H. Rabitz, Phys. Rev. E **82**, 026703 (2010).

[7] T.-S. Ho, H. Rabitz, and S.-I. Chu, Computer Physics Communications **182**, 14 (2011), computer Physics Communications Special Edition for Conference on Computational Physics Kaohsiung, Taiwan, Dec 15-19, 2009.

[8] S. L. Liao, T. S. Ho, S. I. Chu, and H. Rabitz, Phys. Rev. A **84**, 031401 (2011).

[9] S. E. Sklarz and D. J. Tannor, Phys. Rev. A **66**, 053619 (2002).

[10] D. M. Reich, M. Ndong, and C. P. Koch, The Journal of Chemical Physics **136**, 104103 (2012).

[11] S. Boyd and L. Vandenberghe, *Convex optimization* (Cambridge university press, 2004) pp. 215-288

[12] S. Machnes, U. Sander, S. J. Glaser, P. de Fouquières, A. Gruslys, S. Schirmer, and T. Schulte-Herbrüggen, Phys. Rev. A **84**, 022305 (2011).

[13] S. Shi and H. Rabitz, The Journal of Chemical Physics **92**, 364 (1990).

[14] N. Khaneja, T. Reiss, C. Kehlet, T. Schulte-Herbruggen, and S. J. Glaser, Journal of Magnetic Resonance **172**, 296 (2005).

[15] R. Kosloff, Annual Review of Physical Chemistry **45**, 145 (1994).

[16] J. P. Palao and R. Kosloff, Phys. Rev. Lett. **89**, 188301 (2002).

[17] J. P. Palao and R. Kosloff, Phys. Rev. A **68**, 062308 (2003).

[18] A. Borzì, G. Stadler, and U. Hohenester, Phys. Rev. A **66**, 053811 (2002).

[19] U. Hohenester, P. K. Rekdal, A. Borzì, and J. Schmiedmayer, Phys. Rev. A **75**, 023602 (2007).

[20] E. Zahedinejad, S. Schirmer, and B. C. Sanders, Phys. Rev. A **90**, 032310 (2014).

[21] R. Eitan, M. Mundt, and D. J. Tannor, Phys. Rev. A **83**, 053426 (2011).

[22] P. Watts, J. c. v. Vala, M. M. Müller, T. Calarco, K. B. Whaley, D. M. Reich, M. H. Goerz, and C. P. Koch, Phys. Rev. A **91**, 062306 (2015).

[23] M. H. Goerz, G. Gualdi, D. M. Reich, C. P. Koch, F. Motzoi, K. B. Whaley, J. c. v. Vala, M. M. Müller, S. Montangero, and T. Calarco, Phys. Rev. A **91**, 062307 (2015).

[24] F. Yip, D. Mazziotti, and H. Rabitz, The Journal of Chemical Physics **118**, 8168 (2003).

[25] K. Arai and Y. Ohtsuki, Phys. Rev. A **92**, 062302 (2015).

[26] Q. M. Chen and R. B. Wu, "Pulse width modulation for simulating time-dependent quantum systems," e-print arXiv:1607.04054 (2016).

[27] D. G. Holmes and T. A. Lipo, *Pulse width modulation for power converters: principles and practice*, Vol. 18 (Wiley-IEEE Press, 2003).

[28] F. Vasca and L. Iannelli, *Dynamics and Control of Switched Electronic Systems* (Springer London, 2012) pp. 25-61

[29] E. Zahedinejad, J. Ghosh, and B. C. Sanders, Phys. Rev. Lett. **114**, 200502 (2015).

[30] L. M. K. Vandersypen and I. L. Chuang, Rev. Mod. Phys. **76**, 1037 (2005).

[31] A. Castro, M. A. L. Marques, and A. Rubio, The Journal of Chemical Physics **121**, 3425 (2004).

[32] T. M. Zhang, R. B. Wu, F. H. Zhang, T. J. Tarn, and G. L. Long, IEEE Transactions on Control Systems Technology **23**, 2018 (2015).

[33] Q. M. Chen, R. B. Wu, T. M. Zhang, and H. Rabitz, Phys. Rev. A **92**, 063415 (2015).

[34] K. W. Moore, R. Chakrabarti, G. Riviello, and H. Rabitz, Phys. Rev. A **83**, 012326 (2011).

[35] D. V. Zhdanov and T. Seideman, Phys. Rev. A **92**, 052109 (2015).

[36] The CPU time $t_c$ is measured using the *tic* and *toc* commands in *Matlab* 2014*b*.

[37] A. Assion, T. Baumert, M. Bergt, T. Brixner, B. Kiefer, V. Seyfried, M. Strehle, and G. Gerber, Science **282**, 919 (1998).

[38] A. D. Bandrauk and H. Shen, Can. J. Chem. **70**, 555 (1992).